

Modeling Wire Rope Used in Cable Barrier Systems

Cody S. Stolle and John D. Reid
Midwest Roadside Safety Facility
Department of Mechanical Engineering
University of Nebraska-Lincoln
N104 WSEC (0656), Lincoln, NE 68588 USA

Abstract

*An improved LS-DYNA[®] model of 19-mm diameter 3x7 wire rope commonly used in roadside cable guardrail installations has been developed. A Belytschko-Schwer beam element was selected along with material *MAT_MOMENT_CURVATURE_BEAM. Based on physical testing, total axial load vs. true strain and bending moment vs. curvature were generated for use in the model. Since wire rope displays internal damping due to friction of strands and wires, damping was incorporated into the model using the LS-DYNA command *DAMPING_FREQUENCY_RANGE to damp low-frequency bending oscillations. The proposed model was implemented to simulate a dynamic bending test; results compared favorably.*

Introduction

Highway cable barriers have widespread use in the United States, due to the low installation cost, repair time, and ease of construction. Furthermore, highway cable barriers have shown to be effective in reducing the number of cross-median crashes, which are typically high-severity impacts [1].

Developing and testing highway cable barriers is time consuming and expensive. To reduce the time and costs, models of wire rope used in cable guardrail systems have been developed to simulate roadside conditions and impact events. However, wire rope models currently implemented in cable guardrail simulations have typically been developed based on the discretion of the researcher. Component testing of wire rope was not conducted in the development of wire rope models. Bending strength, tensile test data, and dynamic effects were also not considered. Though the models offer a first approximation to the response of the cable barrier system that was similar to physical wire rope, there is need for a more accurate and validated model for use in cable barrier system simulations.

Wire Rope Models

Researchers at the Midwest Roadside Safety Facility (MwRSF) modeled the end terminal of a low-tension three-cable barrier system, and the results were discussed in detail [2-3]. The National Crash Analysis Center (NCAC) modeled wire rope in a V-ditch configuration, and the results were compared to a full-scale test of the system [4]. NCAC also simulated the effects of initial wire rope tension and end anchorage spacing on resulting cable barrier deflection [5].

The existing wire rope models used by MwRSF and NCAC are summarized in Table 1 and depicted in Figure 1. The models consisted of a discrete beam, beam-and-solid, and beam-and-shell approach. Material properties of the new wire rope model are tabulated for comparison.

Table 1. Summary of Modeling Parameters for Wire Rope Models Investigated

Model Name	Components	Materials Used	Linear Mass, ρ_L (kg/mm)	Cross-Sectional Area, A (mm ²)	Modulus of Elasticity, E (GPa)	Bending Resistance, EI (kN-mm ²)
Discrete Beam	Type 6 Discrete Beam	*MAT_CABLE_DISCRETE_BEAM (*MAT_069)	7.3301E-04	154.84	126	0
Beam-and-Solid	Type 6 Discrete Beam	*MAT_CABLE_DISCRETE_BEAM (*MAT_069)	7.3301E-04	154.84	126	0
	Type 15 Two-Point Pentahedron Solid	*MAT_PIECEWISE_LINEAR_PLASTICITY (*MAT_024)	1.3448E-03	255.27	126 / 0.02*	654,838 Fully Elastic 104 Fully Yielded
Beam-and-Shell	Type 1 Hughes-Liu Beam	*MAT_ELASTIC (*MAT_001)	1.3005E-03	283.53	85	543,755
	Type 2 Belytschko-Tsay Shell	*MAT_NULL (*MAT_009)	3.0717E-04	0**	0**	0**
New Wire Rope Model	Type 2 Belytschko-Schwer Beam	*MAT_MOMENT_CURVATURE_BEAM (*MAT_166)	1.2280E-03	154.51	79.9	32,380

* Elastic modulus 126 GPa until 7.94E-5 strain; 0.02 Gpa modulus until 0.5 strain

** Null shells did not contribute to material or section properties

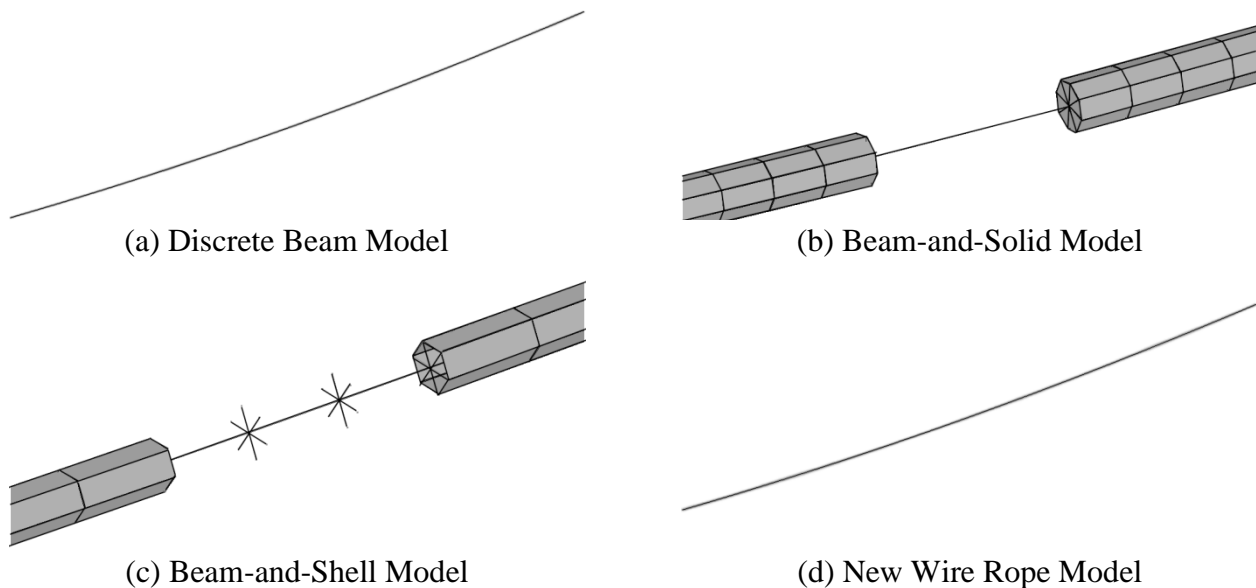


Figure 1. Model Comparison

One of the first models of wire rope implemented in LS-DYNA consisted of type 6 discrete beams defined with *MAT_CABLE_DISCRETE_BEAM material. A modulus of elasticity of 126 GPa was assigned to the beam, and the cable was treated as a perfectly elastic member. It

was observed that the discrete beam model underwent large-amplitude dynamic oscillation and could not sustain compressive loads; thus use of this model was limited.

A ring of solid elements was added to the discrete beam model to provide bending and compressive strength. Eight total pentahedral solid elements were connected to the beams, such that the resulting octagonal solids were inscribed in a circle with a 19-mm diameter. The solid elements incorporated an elasto-plastic material with a modulus of elasticity of 126 GPa. A yield point of 10 MPa and a tangent plastic modulus of 20 MPa were defined to prevent excessive stiffening of the wire rope. Torsional instability, hourglassing, and kinking in the beam-and-solid model were observed, due to the low strength of the solid elements.

Researchers at NCAC used a different modeling method. The beam-and-shell model consisted of a circular rod of 19-mm diameter, with an elastic modulus of 85 GPa. A hexagonal shroud of shell elements were defined with *MAT_NULL material and constrained at each node with nodal rigid bodies to provide a consistent contact surface. Though the model was stable and had little tendency for hourglassing, bending modes and stiffness were not accurate, and non-physical behaviors could be witnessed.

Bogie Testing

Component tests were conducted to analyze the wire rope under dynamic loading conditions and to help develop the cable material model. A surrogate test vehicle with a mass of 772 kg was directed into an initially un-tensioned wire rope connected to two sets of tension load cells mounted to fixed concrete barriers. The test setup is shown in Figure 2. Accelerometers, load cells and high-speed video were used to capture test data.



Figure 2. Dynamic Bending Test DBC-1

An adjustable mount with a cylindrical impact head were fastened to the front of the bogie at the impact height of the wire rope. A lateral catch was welded to the top of the impact head to prevent the wire rope from slipping over the impact head and striking the bogie or the equipment on board. The cylindrical head was projected out from the face of the bogie to prevent dynamic transverse waves from contacting the bogie, which would alter the vibration frequency and tension in the wire rope.

The bogie impacted the center of the wire rope at 6.6 m/s. The maximum tension recorded in the wire rope during the component test was 165.8 kN, and the maximum cable deflection was 975 mm. The bogie vehicle was smoothly decelerated, stopped, and rebounded away from the cable system at 4.4 m/s.

New Wire Rope Model

Though each previous model of wire rope had unique advantages and disadvantages, a universal, consistent model of wire rope was desired which accurately reflected the characteristics of wire rope used in cable guardrail systems. Desired attributes of the new wire rope model included:

1. Simple model construction
2. Accurate tensile and bending properties
3. Accurate wire rope density
4. Element lengths maximizing efficiency and accuracy

After reviewing all available element types implemented in LS-DYNA, it was determined that wire rope most closely resembled a series of beam elements. Though cross-sectional distortions occur due to bending, these distortions are generally very small in a given cross-section and may be ignored. Shear stresses in the rope do not cause changes in wire rope cross-section. Additionally, since the wire rope is nearly circular, torsional and shear stresses do not cause warping.

Two types of beam elements were selected for evaluation, and a variety of material types were applied to the elements. It was determined that the most favorable beam type and material model combination consisted of the type 2 beam element defined with *MAT_MOMENT_CURVATURE_BEAM, or *MAT_166. This little-used resultant material model explicitly declares the axial force in a beam as a function of strain, bending moment as a function of curvature, and torsional resistance as a function of angular twist rate using defined load curves. Other declared variables which may be controlled are summarized in Table 2 and Figure 3.

Wire rope does not have a symmetrical load curve in tension and compression. Because of the helical winding of the wires and strands, the wire rope will act like a compression spring and will unwind when compressed. However, for a 1,000-mm length of wire rope, the critical Euler buckling load is 0.32 kN. With a force level above this, the rope will buckle. Since wire rope has a yield load greater than 50 kN, applying symmetry to the tension-compression curve is sufficient to estimate of the relatively low compressive load that the wire rope will experience.

Torsional properties were estimated, but were inconsequential because the wire rope does not warp with shear or torsional loads. It should be noted that the torque-rate of axial twist curves will not be symmetrical due to the winding differences in wire rope.

Table 2. Relevant Material Parameters, *MAT_MOMENT_CURVATURE_BEAM

Input Variable	Description	Value	Pertinent Information
RO	Density	7.948E-06 kg/mm ³	Divide linear density by cross-sectional area
E	Modulus of Elasticity	200 GPa	Only controls timestep and stress wave transmission
ELAF	Axial Force-Strain Curve	Curve 1	See *DEFINE_CURVE
EPFLG	Evaluation Function Flag	1	0: Nonlinear elastic 1: Multi-linear plastic
CTA, CTB, CTT	Curve Symmetry Flag	0 (all)	0: Curve is symmetric 1: Curve is assymmetric
N(1-8)	Axial Forces to Evaluate Bending, Torque Curves	0, 100 kN	Monotonically increasing values
LCMS(1-8)	Moment-Curvature Curves in S-S Direction	Curve 2 (both N1, N2)	LCMS(1-8) correspond to N(1-8)
LCMT(1-8)	Moment-Curvature Curves in T-T Direction	Curve 2 (both N1, N2)	LCMT(1-8) correspond to N(1-8)
LCT(1-8)	Torque-Rate of Twist Curves	Curve 3 (both N1, N2)	LCT(1-8) correspond to N(1-8)
CFA, CFB, CFT	Dynamic Modification Factors	0.970 Axial 1.1 Bending 1.0 Torque	CFA = Axial CFB = Bending CFT = Torque
HRULE	Hardening Rule	0.0 (isotropic)	Range 0.0 (fully isotropic) to 1.0 (fully kinematic)
REPS	Axial Strain at Rupture	0.046	Based on failure load of 165 kN
RBETA	Torsional Twist Rate at Rupture	1.00E+20	Not measured
RCAPAY, RCAPAZ	Curvature in Y and Z (S and T) Directions at Rupture	1.00E+20	Not measured; not likely to fail in bending

Note: The Curves listed in the Value column are shown in Figure 3.

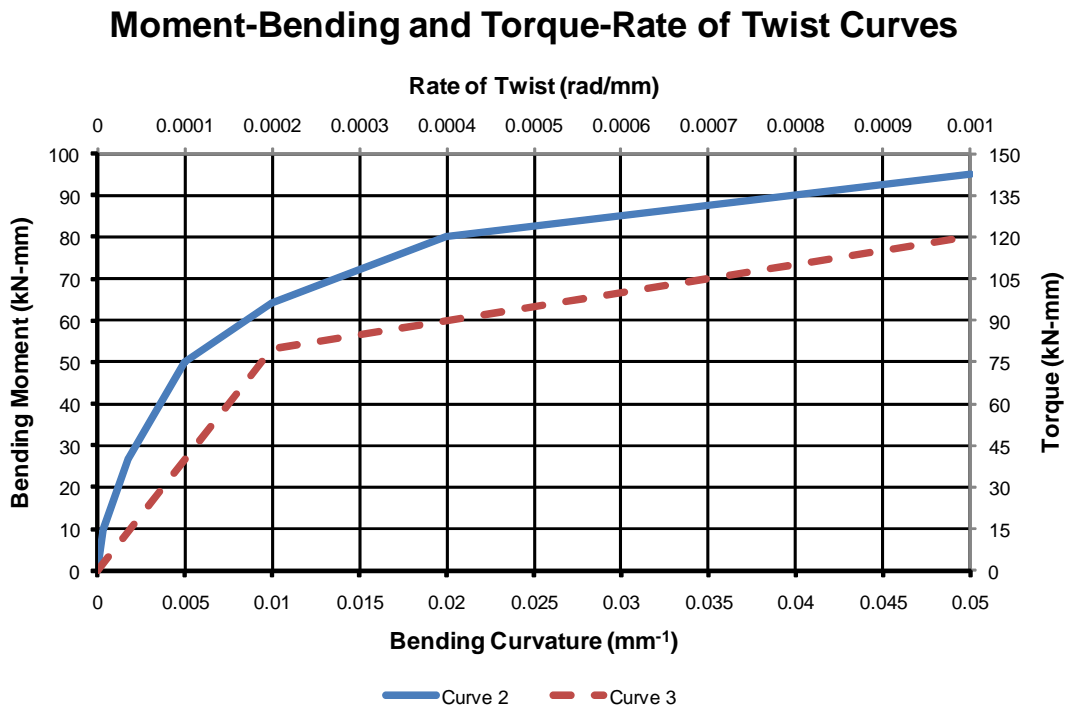
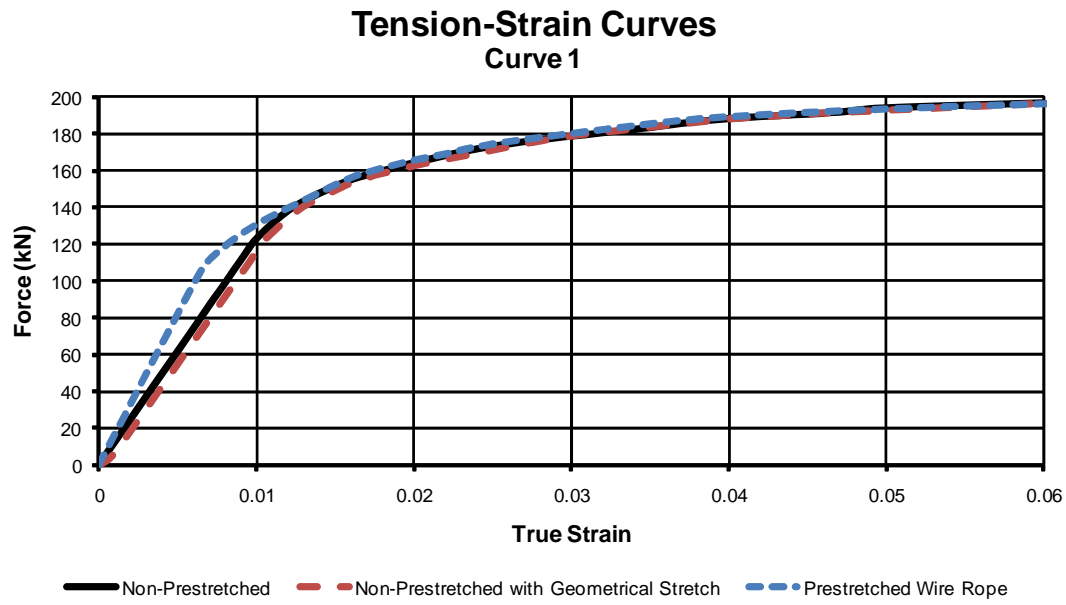


Figure 3. Curves Associated with Table 2.

Damping

In addition to basic material properties, the damping was considered in the new wire rope model. Since wires and strands undergo relative displacement in tension and bending, the *DAMPING_FREQUENCY_RANGE keyword was used to damp vibrations. A damping of 12% was determined to be the most accurate, with an appropriate damped frequency range of 0.1 Hz to 1.0 Hz for a 1,000 mm length of wire rope. As the length of the wire rope increases, the oscillation frequency should decrease linearly with the length; thus the damping frequency range must be scaled with the length of the wire rope to ensure damping in the correct natural bending model. The low damping frequency range is reflective of internal damping in unloaded wire rope, and had the greatest effect just after impact and during the unloading of the simulated wire rope.

Results

A summary of results of the physical test DBC-1 and the simulations of the bogie test is presented in Table 3. Images of DBC-1 and simulation of the new wire model at 200 ms are shown in Figure 4. Loads measured in the cable are shown in Figure 5. Bogie displacements and velocities are shown in Figures 6 and 7, respectively. The new wire rope model compared extremely well with DBC-1 in terms of cable load, bogie displacement and acceleration, and total change in velocity of the bogie. The previous wire rope models did not compare well.

The large differences in the axial forces and bogie behavior predicted using the discrete beam, beam-and-solid, and beam-and-shell methods compared to physical testing rose from the elastic forces in the beams. Since the previous wire rope models were designed only to be used in elastic impact situations, no plasticity data was provided in any of the three models. Whereas these models continued to linearly relate stress and strain throughout the impact event using the modulus of elasticity, the new wire rope model accurately predicted the nonlinear internal force behavior in the beams at higher strains due to the tensile curves coming from test data.

Table 3. Summary of Results

	Maximum Load (kN)	Maximum Displacement (mm)	Maximum Bogie Acceleration (g's)	Change in Velocity (m/s)
Component Test DBC-1	165.8	975	9.49	11.04
New Wire Rope Model	160.9	975	10.25	10.87
Discrete Beam Model	306.4	851	13.35	13.06
Beam-and-Solid Model	266.7	838	14.58	12.81
Beam-and-Shell Model	355.7	714	18.00	14.55

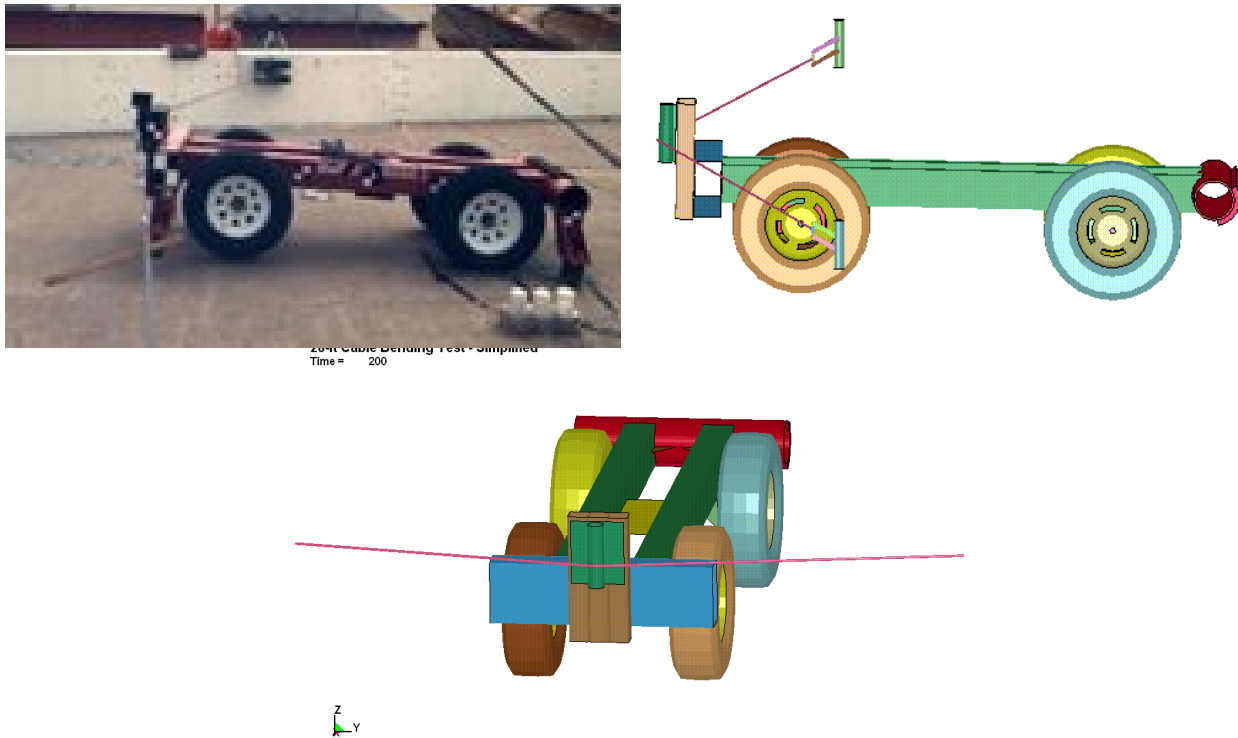


Figure 4. Dynamic Bending at 200 ms

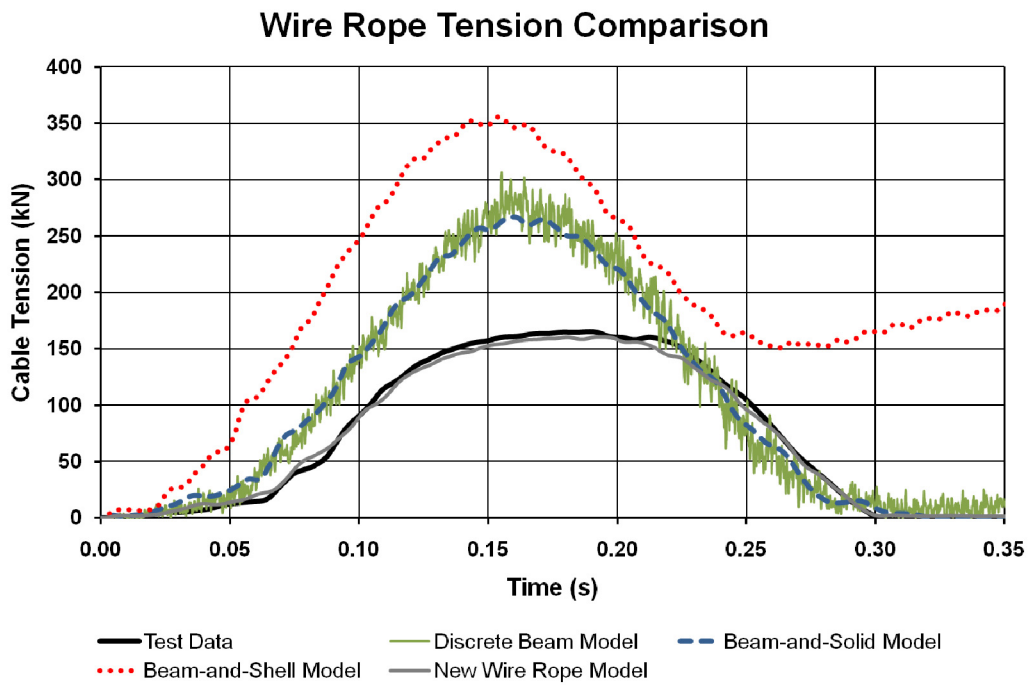


Figure 5. Wire Rope Axial Load

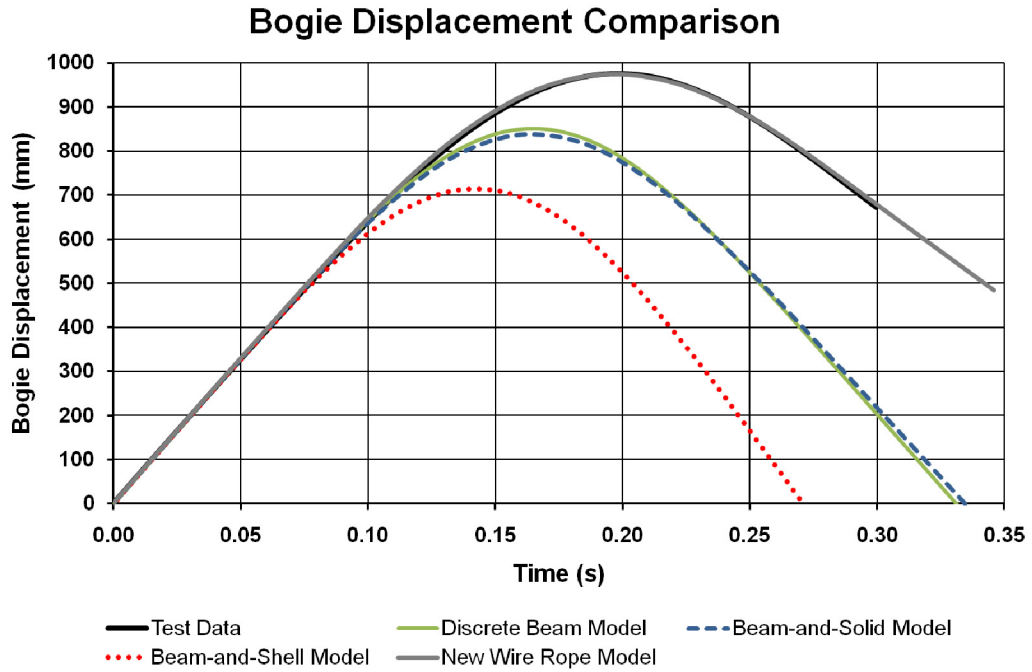


Figure 6. Bogie Displacement

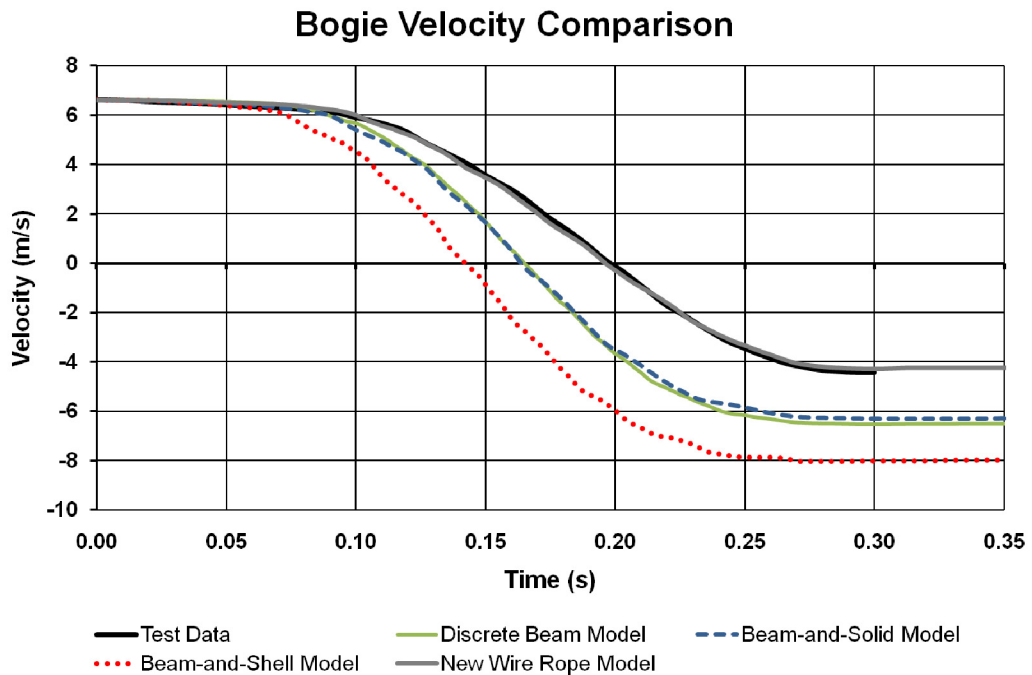


Figure 7. Bogie Velocity

Conclusions

A wire rope model for use in highway cable guardrail simulations was developed based on quasi-static and dynamic component testing. The wire rope model consisted of the type 2 beam element defined with *MAT_MOMENT_CURVATURE_BEAM. A dynamic bending component test of wire rope was modeled using the new wire rope model. The maximum tension in the wire rope, bogie displacement, and resulting velocity in the new wire rope model were within 5% of the component test results; a significant improvement over existing wire rope models. Thus, the new wire rope model is recommended for future analysis on other component testing and for use in full-scale crash test models.

Future Work

Though the new wire rope model is very similar to the behavior of the wire rope observed in component testing, further research is necessary to evaluate the wire rope under high axial strain rates and is necessary for simulating complete cable barrier systems. Further research is also needed to investigate the differences required for modeling prestretched versus non-prestretched wire rope. Finally, since the torsional curve was estimated in this model, a more accurate torsion curve may be necessary for some future applications of highway guardrail wire rope.

Acknowledgments

The authors wish to acknowledge the Midwest Roadside Safety Facility and Livermore Software Technology Corporation for their support. The simulation work performed during this project was completed utilizing the Holland Computing Center of the University of Nebraska–Lincoln. Funding for this research was provided by a grant from the U.S. DOT, University Transportation Centers Program to the Mid-America Transportation Center, at the University of Nebraska.

References

1. Sicking, D.L., de Albuquerque, F.D.B., Lechtenberg, K.A., and Stolle, C.S., "Guidelines for Implementation of Cable Median Barrier," *Transportation Research Record 2120*, Transportation Research Board of the National Academies, Washington D.C., 2009, pp. 82-90.
2. Reid, J.D., Paulsen, T., and Hiser, N.R., "Simulation and Bogie Testing of a New Cable Barrier Terminal," ASME Crashworthiness, Occupant Protection and Biomechanics in Transportation Systems 2003, Paper No. IMECE2003-55104, November 2003.
3. Hiser, N.R., *Slip Base Modeling for Cable Guardrail Systems*, Master's Thesis, Mechanical Engineering, University of Nebraska, Lincoln, NE, April 2003.
4. Marzougui, D., Mohan, P., Kan, C.D., and Opiela, K., "Performance Evaluation of Low-Tension Three-Strand Cable Median Barriers," *Transportation Research Report 2025*, Transportation Research Board of the National Academies, Washington, D.C., 2007.
5. Marzougui, D., "Effects of End-Anchor Spacing and Initial Tension on Cable Barrier Deflection," National Crash Analysis Center, George Washington University, 2008.